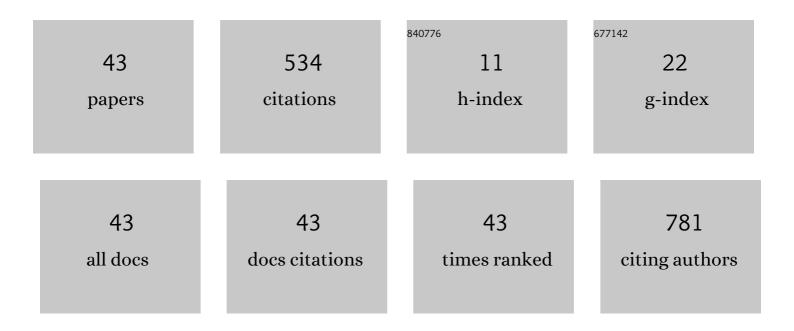
## Andrey S Orekhov

List of Publications by Year in descending order

Source: https://exaly.com/author-pdf/5992787/publications.pdf Version: 2024-02-01



#	Article	IF	CITATIONS
1	Twinâ€jet electropolishing for damageâ€free transmission electron microscopy specimen preparation of metallic microwires. Microscopy Research and Technique, 2021, 84, 298-304.	2.2	3
2	Nanorolls Decorated with Nanotubes as a Novel Type of Nanostructures: Fast Anodic Oxidation of Amorphous Fe–Cr–B Alloy in Hydrophobic Ionic Liquid. ACS Applied Materials & Interfaces, 2021, 13, 2025-2032.	8.0	5
3	Rheology of amorphous olivine thin films characterized by nanoindentation. Acta Materialia, 2021, 219, 117257.	7.9	9
4	Shearing and rotation of β″ and βʹ precipitates in an Al-Mg-Si alloy under tensile deformation: In-situ and ex-situ studies. Acta Materialia, 2021, 220, 117310.	7.9	46
5	Towards ductilization of high strength 7XXX aluminium alloys via microstructural modifications obtained by friction stir processing and heat treatments. Materialia, 2021, 20, 101248.	2.7	9
6	Quantified contribution of β″ and β′ precipitates to the strengthening of an aged Al–Mg–Si alloy. Materials Science & Engineering A: Structural Materials: Properties, Microstructure and Processing, 2020, 774, 138776.	5.6	84
7	Highly oriented graphite produced by femtosecond laser on diamond. Applied Physics Letters, 2019, 114, 251903.	3.3	11
8	Interfacial characteristics and cohesion mechanisms of linear friction welded dissimilar titanium alloys: Ti–5Al–2Sn–2Zr–4Mo–4Cr (Ti17) and Ti–6Al–2Sn–4Zr–2Mo (Ti6242). Materials Characterization, 2019, 158, 109942.	4.4	25
9	In-Situ TEM Stress Induced Martensitic Transformation in Ni50.8Ti49.2 Microwires. Shape Memory and Superelasticity, 2019, 5, 154-162.	2.2	18
10	Crystallization of Thin Copper Films on Silica Substrate for Graphene Growth. Physica Status Solidi (B): Basic Research, 2019, 256, 1800685.	1.5	2
11	Relationship between (micro)structure and functional (photocatalytic and adsorption) properties of anatase–mordenite nanocomposite. Research on Chemical Intermediates, 2019, 45, 2869-2885.	2.7	2
12	Measuring the Local Thickness of Laserâ€Induced Graphitized Layer on Diamond Surface by Raman Spectroscopy. Physica Status Solidi (B): Basic Research, 2019, 256, 1800686.	1.5	8
13	Study of the Q′ (Q)-phase precipitation in Al–Mg–Si–Cu alloys by quantification of atomic-resolution transmission electron microscopy images and atom probe tomography. Journal of Materials Science, 2019, 54, 7943-7952.	3.7	17
14	Design of 2D-nanocrystals in water: preparation, structure and functionalization. Pure and Applied Chemistry, 2018, 90, 833-844.	1.9	2
15	Detonation Nanodiamondâ€Assisted Carbon Nanotube Growth by Hot Filament Chemical Vapor Deposition. Physica Status Solidi (B): Basic Research, 2018, 255, 1700286.	1.5	3
16	Fe–Mo and Co–Mo Catalysts with Varying Composition for Multiâ€Walled Carbon Nanotube Growth. Physica Status Solidi (B): Basic Research, 2018, 255, 1700260.	1.5	26
17	Structure of thermoelectric films of higher manganese silicide on silicon according to electron microscopy data. Semiconductors, 2017, 51, 706-709.	0.5	5
18	Single-Walled Carbon Nanotube Reactor for Redox Transformation of Mercury Dichloride. ACS Nano, 2017, 11, 8643-8649.	14.6	38

ANDREY S OREKHOV

#	Article	IF	CITATIONS
19	The dependence of the microstructure and thermoelectric properties of germanium-doped higher manganese silicide crystals. Semiconductors, 2017, 51, 887-890.	0.5	1
20	Field emission from single-walled carbon nanotubes modified by annealing and CuCl doping. Applied Physics Letters, 2016, 109, .	3.3	5
21	Quasi-two-dimensional diamond crystals: Deposition from a gaseous phase and structural–morphological properties. Physics of the Solid State, 2016, 58, 1458-1462.	0.6	Ο
22	Optical properties and charge transfer effects in single-walled carbon nanotubes filled with functionalized adamantane molecules. Carbon, 2016, 109, 87-97.	10.3	15
23	Structure and mechanical properties of foils made of nanocrystalline beryllium. Crystallography Reports, 2016, 61, 549-557.	0.6	4
24	Electron microscopy study of the microstructure of Ni–W substrate surface. Crystallography Reports, 2016, 61, 1002-1007.	0.6	0
25	Structural peculiarities of single crystal diamond needles of nanometer thickness. Nanotechnology, 2016, 27, 455707.	2.6	12
26	Electron microscopy characterization of higher manganese silicide film structure on silicon. Nanotechnologies in Russia, 2016, 11, 610-616.	0.7	8
27	High-resolution X-ray diffractometry and transmission electron microscopy as applied to the structural study of InAlAs/InGaAs/InAlAs multilayer transistor nanoheterostructures. Journal of Surface Investigation, 2016, 10, 495-509.	0.5	1
28	Diamond platelets produced by chemical vapor deposition. Diamond and Related Materials, 2016, 65, 13-16.	3.9	10
29	Microstructure of the Al-La-Ni-Fe system. Crystallography Reports, 2015, 60, 23-29.	0.6	10
30	Study of doped higher manganese silicides crystals by transmission electron diffraction and electron backscatter diffraction. Crystallography Reports, 2014, 59, 78-87.	0.6	5
31	The isolated flat silicon nanocrystals (2D structures) stabilized with perfluorophenyl ligands. Journal of Nanoparticle Research, 2014, 16, 1.	1.9	12
32	Stabilization of nanocrystalline 2D structures of silicon with perfluorophenyl ligands. Russian Journal of Coordination Chemistry/Koordinatsionnaya Khimiya, 2014, 40, 1-4.	1.0	5
33	Electrophysical characteristics and structural parameters of metamorphic HEMT nanoheterostructures In0.7Al0.3As/In0.7Ga0.3As/In0.7Al0.3As containing superlattices with different numbers of periods in the metamorphic buffer. Crystallography Reports, 2014, 59, 425-429.	0.6	2
34	Study of structural order in porphyrin-fullerene dyad ZnDHD6ee monolayers by electron diffraction and atomic force microscopy. Crystallography Reports, 2013, 58, 927-933.	0.6	5
35	SEM/EDS/EBSD study of the behaviour of Ge, Mo and Al impurities in complex-doped crystals of higher manganese silicide. Journal of Physics: Conference Series, 2013, 471, 012016.	0.4	0
36	Comparison of the data of X-ray microtomography and fluorescence analysis in the study of bone-tissue structure. Crystallography Reports, 2012, 57, 700-707.	0.6	7

ANDREY S OREKHOV

#	Article	IF	CITATIONS
37	The Study of Nb3Sn Phase Content and Structure Dependence on the Way of Ti Doping in Superconductors Produced by Bronze Route. Physics Procedia, 2012, 36, 1510-1515.	1.2	11
38	Microstructure of eutectic composites Ln 1â^'x Ln′ x MnO3 (Ln = Eu or Tb; Ln′ = Y or Ho) near the transition between the orthorhombic structure and hexagonal structures. Crystallography Reports, 2012, 57, 549-554.	0.6	0
39	Size-induced effects in gallium selenide electronic structure: The influence of interlayer interactions. Physical Review B, 2011, 84, .	3.2	100
40	Mn4Si7-Si〈Mn〉-Mn4Si7 and Mn4Si7-Si〈Mn〉-M photodiodes. Technical Physics, 2011, 56, 1423-14	42 <b>8.</b> 7	6
41	On the growth of higher manganese silicide films on silicon. Technical Physics, 2010, 55, 874-876.	0.7	2
42	About the Interface Between the Higher Manganese Silicide Film and Si (111). , 2006, , .		0
43	Investigation of the Magnesium Silicide Mg <sub>2</sub> Si Films. , 2006, , .		Ο